CONF-8810155--22

INITIAL ASSESSMENT OF THE PROCESSES AND SIGNIFICANCE OF THERMAL AGING IN CAST STAINLESS STEELS*

O. K. Chopra and H. M. Chung

Materials and Components Technology Division
Argonne National Laboratory
Argonne, Illinois 60439

CONF-8810155--22

DE89 003633

October 1988

DISCLAIMER

To be presented at the 16th Water Reactor Safety Information Meeting, October 24-27, 1988, National Bureau of Standards, Gaithersburg, MD.

*Work supported by the Office of Nuclear Regulatory Research, U. S. Nuclear Regulatory Commission.

INITIAL ASSESSMENT OF THE PROCESSES AND SIGNIFICANCE OF THERMAL AGING IN CAST STAINLESS STEELS*

O. K. Chopra and H. M. Chung

Materials and Components Technology Division
Argonne National Laboratory
Argonne, Illinois 60439

Abstract

Charpy-impact and J-R curve data for thermally aged cast stainless steel are presented. The effects of material variables on the embrittlement of cast materials are evaluated. The chemical composition and ferrite morphology have a strong effect on the kinetics and extent of embrittlement. The procedure and correlations for predicting the impact strength and fracture toughness of cast component during reactor service are described.

1. Introduction

A program is being conducted to investigate the significance of low-temperature embrittlement of cast duplex stainless steels under LWR operating conditions and to evaluate possible remedies to the embrittlement problem for existing and future plants. The scope of the investigation includes the following goals: (1) characterize and correlate the microstructure of in-service reactor components and laboratory-aged material with loss of fracture toughness to establish the mechanism of aging and to validate the simulation of in-reactor degradation by accelerated aging, (2) establish the effects of key compositional and metallurgical variables on the kinetics and extent of embrittlement, and (3) obtain fracture toughness data on long-term-aged materials to predict the degree of toughness loss suffered by cast

*RSR FIN Budget No. A2243; RSR Contact: J. Muscara.

stainless steel components during normal and extended service life of reactors.

Microstructural and mechanical properties data are being obtained on 19 experimental heats (static-cast keel blocks) and 6 commercial heats (centrifugally cast pipes and a static-cast pump impeller and pump casing ring) as well as reactor-aged material of CF-3, CF-8, and CF-8M grades of cast stainless steel. Six of the experimental heats are also in the form of 76-mm-thick slabs. The reactor-aged material is from the recirculating cover plate assembly of the KRB reactor, which was in service for ~12 yrs (~8 yr at service temperature of 284°C). Fractured impact test bars from five heats of aged cast stainless steel were obtained from Georg Fischer Co. (GF), Switzerland, for microstructural characterization. The materials are from a previous study of long-term aging behavior of cast stainless steel.[1] The data on chemical composition, ferrite content, hardness, ferrite morphology, and grain structure of the experimental and commercial heats have been reported earlier.[2-6] The chemical composition, hardness, and ferrite content and distribution of some of the cast materials are given in Table 1. Specimen blanks for Charpy-impact, tensile, and J-R curve tests are being aged at 290, 320, 350, 400, and 450°C for times up to 50,000 h. This paper presents an analysis of the mechanical property data for several heats of cast stainless steel aged for up to 30,000 h.

2. Charpy-Impact Tests

Impact tests were conducted on standard Charpy V-notch specimens machined from the aged and unaged materials according to ASTM specification E 23. A Dynatup Model 8000A drop weight impact machine with an instrumented tup and data readout system was used for the tests. The data for room temperature

impact energy were analyzed to determine the kinetics and extent of embrittlement. The Charpy-impact energy, KCV, is expressed as,

$$KCV = K_m + \beta\{1 + \tanh [(P - \theta)/\alpha]\} , \quad (1)$$

where P is the aging parameter, K_m is the minimum impact energy reached after long-term aging, β is half the maximum decrease in impact energy (i.e., half the difference between initial and minimum impact energy), θ is the log of the time to achieve β reduction in impact energy, and α is a shape factor representing the time between the start and end of the decrease in impact energy. The time, t, at different aging temperatures is expressed by an Arrhenius relationship given by,

$$t = 10^P \exp\left[\frac{Q}{R}\left(\frac{1}{T} - \frac{1}{673}\right)\right] , \quad (2)$$

where Q is the activation energy, R the gas constant, and T the absolute temperature. The aging parameter, P, which represents the degree of aging reached after 10^P h at 400°C.

The values of the constants in Eqs. (1) and (2) for various heats of cast stainless steel are given in Table II and the best fit curves for some of the heats are shown in Figs. 1-3. The Charpy-impact data are plotted as a function of the aging parameter in Figs. 4-6. The actual time and temperature of aging are shown on five separate axes below the figures. The service time, in years, at the hot-leg temperature of LWRs is shown at the top of the figure.

The effect of aging temperature and time on the shifts in upper-shelf energy (USE) and transition temperature of the three grades of cast material are shown in Figs. 7 and 8. The impact energy data were analyzed with the

hyperbolic tangent function given by

$$KCV = K_o + B\{1 + \tanh [(T-C)/D]\} , \quad (3)$$

where K_o is the lower-shelf energy, T is the test temperature, B is half the distance between upper- and lower-shelf energy, C is the mid-shelf transition temperature in °C, and D is the half width of the transition region. The values of B, C, and D change with aging time whereas K_o is assumed to be unaffected by aging. The best-fit curves for the different heats and aging conditions are shown in Figs. 7 and 8 and the values of the constants are given in Table III.

The results indicate that thermal aging decreases the impact energy and shifts the ductile-to-brittle transition curves to higher temperatures. However, different heats exhibit different degrees of embrittlement. In general, the low-carbon CF-3 grades of cast materials are the most resistant, and the molybdenum-containing CF-8M grades are least resistant to embrittlement. For all grades of cast materials, the extent of embrittlement increases with an increase in ferrite content. The significant results are summarized below.

(a) High-carbon CF-8 stainless steels exhibit low lower-shelf energy and high mid-shelf transition temperature relative to the low-carbon CF-3 steels. The lower impact energy for CF-8 steels is attributed to $M_{23}C_6$ carbides which form at the ferrite/austenite phase boundaries, during the production heat treatment of the casting. The presence of large carbides weakens the phase boundaries, and the fracture mode in the lower-shelf or transition regime is predominantly phase boundary separation and cleavage of

the ferrite.[7,8] In contrast, the CF-3 steels show a dimpled ductile failure at all test temperatures.

(b) The mid-shelf transition temperature of unaged CF-8M steels is lower than that of unaged CF-8 steels. The difference is due to the absence of phase boundary carbides in the as-cast material. Fracture by phase boundary separation is observed in only a few heats of CF-8M steel, depending on whether or not the material contained phase boundary carbides.

(c) Additional precipitation of phase boundary carbides and/or growth of existing carbides occurs in the high-carbon steels during aging at 450 or 400°C.[8] The fracture mode of Charpy-impact specimens aged at 450°C and tested at low temperatures, i.e., below the transition temperature, was predominantly phase boundary separation. Although phase boundary carbides are not present in the as-cast CF-8M material, they form during aging.

(d) Phase boundary carbides have a strong influence on the transition temperature, but have little or no effect on USE, e.g., transition curves for heats 68 and 69 in Fig. 7. The presence of carbides at the phase boundaries leads to phase boundary separation and/or initiation of cleavage of the ferrite at low temperatures, while ductile fracture at high temperatures, by void formation and growth, is not influenced by the phase boundary carbides.

(e) The results suggest a "saturation effect" for USE after aging. For example, the values of USE decrease significantly after aging for 2600 h at 400°C and do not change for longer aging times, Fig. 8. This behavior is observed for all grades of material.

(f) Thermal aging leads to a decrease in the ferrite content of all grades of cast stainless steel, Fig. 9; particularly after aging 450°C. The decrease in ferrite content for CF-8M steels is significantly greater than for the other grades. Microstructural studies[9,10] indicate that aging of cast stainless steels at temperatures below 500°C leads to the formation of chromium-rich α' phase, nickel- and silicon-rich G phase, and γ_2 austenite in the ferrite and $M_{23}C_6$ carbides at the phase boundaries. The ferrite phase typically contains ~26% Cr and 5% Ni. The formation of α' or carbides depletes the matrix of chromium which leads to the transformation of ferrite to austenite. The larger decrease for CF-8M steels and for 450°C aging may be attributed to the formation and/or growth of phase boundary carbide. The migration of phase boundaries is often observed in aged CF-8M steels.

(g) Charpy-impact data for CF-3 and some CF-8M steels indicate an inversion in impact energy at temperatures in the transition region, i.e., impact energy of samples aged at 450°C is higher than of those aged for equivalent times at 400 or 350°C. For example, the mid-shelf transition temperature (constant C in Table III) for heats 69 and 75, aged for 2570 h at 450°C, is lower than that after aging at 400°C for the same time. Furthermore, the room temperature impact energies of heats 52, 47, 51, and P2, aged for 10,000 h at 450°C, were 10 to 15% higher than after aging for 10,000 h at 400°C. This behavior was observed for cast materials which do not contain phase boundary carbides and have a very low mid-shelf transition temperature in the unaged condition, i.e., for most of the low carbon CF-3 grades and some CF-8M grades of cast stainless steel.

(h) The kinetics of embrittlement vary significantly for the various heats of cast stainless steel; the activation energies range between 20 and 56 kcal/mole. The activation energy is lower for the molybdenum-containing CF-8M steels or for steels containing higher nickel content. The values of activation energy obtained in the present study are significantly higher than those observed in the Georg Fischer study,[1] e.g., activation energies between 17 and 25 kcal/mole.

(i) The shape of the impact energy vs aging time curves also varies considerably for the various heats, e.g., shape factor α varies between ~0.6 and 1.7.

These results indicate that the kinetics and extent of embrittlement are controlled by several mechanisms which depend on material parameters and aging temperature. Data obtained at 450°C aging are not representative of reactor operating conditions; materials aged at 450°C show significant precipitation and growth of phase boundary carbides and a large decrease in ferrite content of the material. Consequently, extrapolation of the 450°C data to predict the extent of embrittlement at reactor temperatures may not be valid.

The results also indicate that the current "best estimates" of the kinetics of embrittlement are not accurate. The activation energy for the process of embrittlement is currently described as a function of the chemical composition of the cast material,[11] given by

$$Q(\text{kcal/mole}) = -43.64 + 4.76(\%\ \text{Si}) + 2.65(\%\ \text{Cr}) + 3.44(\%\ \text{Mo}). \qquad (3)$$

The activation energy from Eq. (3) ranges between 15 and 25 kcal/mole for the various grades of cast stainless steels. These values are significantly lower than those observed in the present study. Consequently, the predictions based on Eq. (3) will be conservative for most heats of cast stainless steel. For example, extrapolation of a 40 yr reactor lifetime at 320°C based on activation energy of 20 or 45 kcal/mole, is equivalent to 47,000 or 3700 h at 400°C, respectively. Figures 5 and 6 show that for the CF-8 and CF-3 steels, the minimum impact energy is not reached during the reactor lifetime. However, Eq. (3) may be nonconservative for some heats of cast stainless steel since it does not include the effects of other elements, such as nickel, carbon, and nitrogen, on the kinetics of embrittlement.

3. Kinetics of Embrittlement

The kinetics data from Framatome,[11] Georg Fischer,[1] and the present study were analyzed to develop a correlation between the activation energy for embrittlement and the chemical composition of the cast material. Initially, all major elements and carbon and nitrogen were included in the correlation. Elements with poor coefficient of correlation were then excluded. The analyses yielded two separate correlations: one for the Argonne and Framatome data, given by

$$Q(\text{kcal/mole}) = 21.64 + 2.30\ Cr - 1.94\ Ni - 1.8\ Mo + 4.92\ Si - 29.40\ Mn + 75.93\ N \qquad (4)$$

and the other for the Georg Fischer data, give by,

$$Q(\text{kcal/mole}) = -15.93 + 1.65\ Cr - 1.30\ Ni + 1.93\ Mo + 4.10\ Si + 10.54\ Mn + 71.00\ N. \quad (5)$$

The observed and predicted activation energies for the two data sets are plotted in Fig. 10. The coefficients for Cr, Ni, Si, and N show the same behavior in the two correlations, however, the constant and the coefficients for Mo and Mn have opposite sign.

Equation (4) represents a wide range of material composition and was used to predict the activation energy for embrittlement of two heats of cast material not used in obtaining the correlation. The impact energies for the heats are plotted as a function of aging parameter in Fig. 11. The data obtained for different aging temperatures follow a single curve. The results indicate that for both heats, the minimum values of impact energy will be reached within the reactor lifetime of 40 yr.

The different effects of constituent elements in the two correlations are not clearly understood. In binary Fe-Cr alloys, an increase in Cr content is known to decrease the time for α' formation.[12] N also enhances Cr clustering.[13,14] The positive sign for the coefficients for Cr and N indicates that such effects are greater at high temperatures. These elements also influence the precipitation of carbides, nitrides, or carbonitrides. Precipitation of carbides or nitrides occurs primarily at 450 or 400°C and is extremely low at lower temperatures. Consequently, the formation of phase boundary carbides would increase the activation energy for embrittlement.

The influence of other elements, most likely, is on the precipitation of G phase, a multicomponent phase consisting of Ni, Si, Cr, Mo, Fe, and some Mn and C. Microstructural studies[9,10] indicate that G-phase precipitation decreases the activation energy for embrittlement. However, the effect of

constituent elements on G-phase precipitation is not known. Limited data[15,16] suggest that the composition of G phase may change with aging temperature. For example, the G phase observed in two similar heats of CF-8M steels aged at 400 and 450°C consisted of ~25% Ni and ~14% Mo, but the Si and Cr contents were 14 and 25% at 450°C and 28 and 12% at 400°C. The effect of material composition on G-phase precipitation needs to be established to better understand and develop a single correlation for the kinetics of embrittlement.

4. Extent of Embrittlement

The Charpy-impact data were analyzed to obtain a correlation between the extent of embrittlement (i.e., minimum impact energy, K_m, achieved after long-term aging) and material variables. The minimum impact energy is plotted in Fig. 12 as a function of a material parameter consisting of the measured ferrite content (δ_m in %); Cr, Mo, Si, C, and N content (in %) of the steel; and the mean ferrite spacing (ℓ in μm). The results for all heats for which the material variables were known are shown in the figure. The data show a good correlation with the material parameter. The results indicate that the impact energy will be less than 50 J/cm^2 (~30 ft·lb) for those cast stainless steels for which the material parameter is greater than ~60.

For cast stainless steels containing >10% ferrite, the mean ferrite spacing is in the range of 40 to 200 μm; Cr + Mo + Si concentration is ~22% for CF-8 or CF-3 and ~24% for CF-8M; and N content is typically 0.04%. Thus, for cast materials with 0.6% C and 100 μm ferrite spacing, the impact energy will be below 50 J/cm^2 when the ferrite content is above 20%. Cast materials with 10 or 15% ferrite can also reach very low impact strength when the ferrite spacing or the nitrogen content is high.

For all cast stainless steels in service, the variables in the material

parameter are readily available. The composition is known, ferrite content can be calculated from the composition or measured with a ferrite scope, and the ferrite spacing can be determined from surface replica technique. Thus, Fig. 12 can be used to estimate the extent of embrittlement for any cast stainless steel component.

5. J-R Curves

The results of the J-R curve tests[17] indicate that thermal aging decreases J_{IC} and Tearing modulus of cast stainless steel at room temperature as well as at 290°C. The reduction in toughness is greater for materials aged at 400 or 450°C than for those aged at 350°C for similar lengths of time. The fracture toughness of the high-carbon CF-8 steels is lower than for the low-carbon CF-3 steels. After aging for 9980 h at 400°C, the J_{IC} value for heat P1 (CF-8 grade) at room temperature decreased from 2171 to 254 kJ/m^2, and the tearing modulus decreased from 546 to 200.

The fracture toughness results are consistent with the Charpy-impact data, i.e., unaged and aged materials that show low impact strength also exhibit lower fracture toughness. The J_{IC} values and Charpy V-notch impact energies obtained at room temperature and at 290°C are plotted in Fig. 13. Results from the studies at Westinghouse (WH),[19] Electric Power Research institute (EPRI),[18] and FRA[11] are also shown. The dashed lines represent the lower bound values. Thermal aging decreases the J_{IC} values, and the relative reductions in J_{IC} are similar to the relative decreases in impact energy. Figure 12 shows that the minimum impact energy can be as low as 20 J/cm^2 for some heats of cast stainless steel. The corresponding J_{IC} value from the lower band curve in Fig. 13a would be ~40 kJ/m^2. Thus, the correlations in Figs. 12 and 13 can be used to predict the minimum J_{IC} values for any heat of

cast stainless steel aged for long times.

The Tearing modulus also decreases with thermal aging. The Tearing modulus and J_{IC} value for various heats and aging conditions are shown in Fig. 14. At both test temperatures, the Tearing modulus decreases with a decrease in J_{IC}. Fracture toughness data for other aging conditions as well as other heats are being obtained to better establish the correlation between J_{IC}, Tearing modulus, and Charpy-impact energy.

6. Assessment of Embrittlement under LWR Conditions

The embrittlement of any cast stainless steel component during reactor service can be estimated from Fig. 12 and Eqs. (1), (2), and (4). The material information needed for the assessment is the chemical composition, ferrite content and spacing, and initial impact strength of the cast material. Knowing the material parameter, the minimum room temperature impact energy, K_m, is determined from Fig. 12. The constant β is obtained from the difference between the initial and minimum values of impact energy and the activation energy, Q, is determined from Eq. (4). The average values of the constants Q and α in Eq. (1) are 2.8 and 1.0, respectively. The decrease in impact energy during service at reactor temperature is determined from Eqs. (1) and (2).

Examples of the predicted embrittlement behavior of heats susceptible to embrittlement (A and C) and typical heats (B and D) of CF-8M and CF-8 cast stainless steel are shown in Fig. 15. The theoretical chemical composition and the ferrite content and spacing of the heats are given in Table IV. All compositions are within ASTM specifications. The compositions of heats A and C are selected to give high ferrite content and fast kinetics of embrittlement (i.e., low activation energy). The mean ferrite spacing for most cast

stainless steels with >10% ferrite varies between 40 and 200 μm. A large value of the ferrite spacing is selected for heats A and C to get a conservative estimate of the extent of embrittlement.

The results show that the impact energy of heats A and C will decrease below 40 J/cm^2 (~20 ft·lb) after 4 or 5 yr service at 320°C. Heats B and D with lower ferrite content (15%) exhibit much less embrittlement, i.e., the impact energy will not decrease below 90 J/cm^2 even after long-time service. The kineitcs of embrittlement are also slower for these heats; the activation energy is >40 kcal/mole compare to 18 kcal/mole for heats A and C. The results also show that the minimum impact energy is the important factor in estimating the embrittlement behavior. Slow kinetics of embrittlement, i.e., high activation energy, delay the decrease in impact strength, but the material reaches the lowest value of impact strength near the end of reactor lifetime. This behavior is seen for heat E which has the same material parameters as heat C, but the activation energy was assumed to be 45 kcal/mole rather than the calculated value of 18 kcal/mole. Even with very slow kinetics, the impact energy decreases to ~40 J/cm^2 after 40 yr of service.

The decrease in fracture toughness, i.e., values of J_{IC} and Tearing modulus, during reactor service can be estimated using the room temperature impact energy and Figs. 13 and 14. For example, an impact energy of 25 J/cm^2 corresponds to a lower bound value of 70 kJ/m^2 for J_{IC}. The Tearing modulus can be estimated from Fig. 14; however, the correlations between J_{IC} and Tearing modulus are not well established at present.

7. Recovery Anneal

The low-temperature embrittlement of cast stainless steel can be reversed by annealing at 550°C for 1 h.[8] The ductile-to-brittle transition curves for

the KRB pump cover plate material, after reactor service and after reannealing for ~1 h at 550°C, are shown in Fig. 15. The results show that the upper-shelf energy of the material increases from 247 to 330 J/cm^2 after reannealing and the mid-shelf transition temperature decreases from 37 to -16°C. Microstructural characterization of the reactor-aged material showed α' and G phases in the ferrite matrix and large carbides at the phase boundaries.[9,10] The α' phase is unstable at 550°C and thus dissolves after annealing. The reannealed material showed no α'; however, the size and distribution of the G phase were essentially the same as in the reactor-aged material.[9,10] These results indicate that the primary mechanism for embrittlement is the formation of α' phase.

The annealed material was aged at 320, 350, and 400°C to investigate the reembrittling behavior. The results are shown in Fig. 16. The material reembrittles in a relatively short time. For example, aging for 100 h at 400°C or 3000 h at 320°C, decreased the impact energy to the value observed after reactor service. After 3000 h of aging at 400°C, the impact energy decreased to ~20 J/cm^2, a value close to the lower-shelf energy for the material.

It is not clear at present whether this behavior is typical of all reannealed cast stainless steels or is unique to this material. Recovery annealed material from other heats and grades of cast stainless steel are being aged to better establish the reembrittlement behavior.

7. Conclusions

Charpy-impact and J-R curve data for thermally aged cast stainless steel are presented. The effects of material variables on the embrittlement of cast materials are evaluated. The results show that the material composition and

the ferrite content and spacing are important parameters in controlling the kinetics and extent of embrittlement. The ferrite morphology has a strong effect on the extent of embrittlement while the material composition influences the kinetics of embrittlement. The results indicate that the kinetics of embrittlement can vary significantly with the composition of the cast material.

Mechanical property results from the present study and data from other investigations were analyzed to develop the procedure and correlations for predicting the kinetics and extent of embrittlement under reactor operating conditions, from the material parameters. The method and examples of estimating the room temperature impact strength and fracture toughness of cast components during reactor service are described. Correlations for predicting the toughness loss at reactor temperatures are also being developed. Mechanical tests are in progress on long-term laboratory-aged material and reactor-aged material to validate and/or modify the correlations.

7. Acknowledgments

This work was supported by the Office of Nuclear Regulatory Research, U. S. Nuclear Regulatory Commission. The authors are grateful to A. Sather, G. M. Dragel, C. Ensel, and W. K. Soppet for conducting the mechanical tests and to G. M. Dragel for experimental contributions.

References

1. A. Trautwein and W. Gysel, "Influence of Long Time Aging of CF-8 and CF-8M Cast Steel at Temperatures Between 300 and 500°C on the Impact Toughness and the Structure Properties," Spectrum, Technische

Mitteilungen aus dem+GF+Konzern, No. 5, May 1981; Stainless Steel Castings, V. G. Behal and A. S. Melilli, eds., ASTM STM 756, p. 165 (1982).

2. O. K. Chopra and H. M. Chung, Long-Term Embrittlement of Cast Duplex Stainless Steels in LWR Systems: Annual Report, October 1983-September 1984, NUREG/CR-4204, ANL-85-20, March 1985; Nucl. Eng. Des., 89, 305 (1985).

3. O. K. Chopra and H. M. Chung, Long-Term Embrittlement of Cast Duplex Stainless Steels in LWR Systems: Annual Report, October 1984-September 1985, NUREG/CR-4503, ANL-86-3, January 1986.

4. O. K. Chopra and H. M. Chung, Long-Term Embrittlement of Cast Duplex Stainless Steels in LWR Systems: Semiannual Report, October 1985-March 1986, NUREG/CR-4744 Vol. I, No. 1, ANL-86-54, September 1986.

5. O. K. Chopra and G. Ayrault, in Materials Science and Technology Division Light-Water-Reactor Safety Research Program: Quarterly Progress Report, October-December 1983, NUREG/CR-3689 Vol. IV, ANL-83-85 Vol. IV, pp. 129-151 (August 1984).

6. O. K. Chopra and H. M. Chung, in Materials Science and Technology Division Light-Water-Reactor Safety Materials Engineering Research Programs: Quarterly Progress Report, January-March 1984, NUREG/CR-3998 Vol. I, ANL-84-60 Vol. I, p. 52 (September 1984).

7. O. K. Chopra and H. M. Chung, in Environmental Degradation of Materials in Nuclear Power Systems-Water Reactors, G. J. Theus and J. R. Weeks, eds., The Metallurgical Society, p. 737 (1988).

8. O. K. Chopra and H. M. Chung, in Properties of Stainless Steels in Elevated Temperature Service, M. Prager, ed., MPC-Vol. 26/PVP-Vol. 132, ASME, p. 79 (1988).

9. H. M. Chung and O. K. Chopra, in Properties of Stainless Steels in Elevated Temperature Service, M. Prager, ed., MPC-Vol. 26/PVP-Vol. 132, ASME, p. 17 (1988).

10. H. M. Chung and O. K. Chopra, in Proc. Second Intl. Symp. on Environmental Degradation of Materials in Nuclear Power Systems-Water Reactors, September 9-12, 1985, Monterey, CA, American Nuclear Society, LaGrange Park, IL, pp. 287-292 (1986).

11. G. Slama, P. Petrequin, and T. Magep, "Effect of Aging on Mechanical Properties of Austenitic Stainless Steel Castings and Welds," presented at SMIRT Post-Conference Seminar 6, Assuring Structural Integrity of Steel Reactor Pressure Boundary Components, August 29-30, 1983, Monterey CA.

12. P. J. Grobner, Metall. Trans. 4, 251 (1973).

13. R. Langneborg, Trans. ASM 60, 67 (1967).

14. A. Hendry, Z. F. Mazur, and K. H. Jack, Metal Science 13, 482 (1979).

15. M. K. Miller, J. Bentley, S. S. Brenner, and J. A. Spitznagel, in Proc. 43rd Annual Meeting Electron Microscopy Society of America, ed. G. W. Bailey, San Francisco Press, p. 328 (1985).

16. M. Vrinat, R. Cozar, and Y. Meyzaud, Scripta Met. 20, 1101 (1986).

17. A. L. Hiser, Tensile and J-R Curve Characterization of Thermally Aged Cast Stainless Steels, NUREG/CR-5024, MEA-2229, September 1988.

18. P. McConnell and J. W. Sheckherd, "Fracture Toughness Characterization of Thermally Embrittled Cast Duplex Stainless Steel," EPRI Report NP-5439, March 1987.

19. E. I. Landerman and W. H. Bamford, in Ductility and Toughness Considerations in Elevated Temperature Service, ASME MPC-8, p. 99 (1988).

TABLE I. Product Form, Chemical Analysis, Hardness, and Ferrite Morphology of Various Heats of Cast Stainless Steel

Heat	Grade	Product Form	Size (mm)	Composition (wt %)							Hardness R_B	Ferrite Content (%)		Ferrite Intercept (μm)
				C	N	Mn	Si	Ni	Cr	Mo		Calc.	Meas.	
59	CF-8	Keel B.	180 x 120 x 30-90	0.062	0.045	0.60	1.08	9.34	20.33	0.32	83.2	8.8	13.5	75
61	CF-8			0.054	0.080	0.65	1.01	8.86	20.65	0.32	85.2	10.0	13.1	82
60	CF-8			0.064	0.058	0.67	0.95	8.34	21.05	0.31	86.7	15.1	21.1	63
47	CF-3			0.018	0.028	0.60	1.06	10.63	19.81	0.59	79.6	8.4	16.3	68
52	CF-3			0.009	0.052	0.57	0.92	9.40	19.49	0.35	81.6	10.3	13.5	69
51	CF-3			0.010	0.058	0.63	0.86	9.06	20.13	0.32	83.8	14.2	18.0	52
63	CF-8M			0.055	0.031	0.61	0.58	11.85	19.37	2.57	81.5	6.4	10.4	81
65	CF-8M			0.049	0.064	0.50	0.48	9.63	20.78	2.57	89.9	20.9	23.4	43
64	CF-8M			0.038	0.038	0.60	0.63	9.40	20.76	2.46	89.7	28.9	28.4	35
P1	CF-8	Pipe	890 OD 63 wall	0.036	0.056	0.59	1.12	8.10	20.49	0.04	84.9	17.7	24.1	90
P2	CF-3	Pipe	930 OD 73 wall	0.019	0.040	0.74	0.94	9.38	20.20	0.16	83.8	12.4	15.6	69
I	CF-3	Impeller	930 OD 73 wall	0.019	0.032	0.47	0.83	8.65	20.14	0.45	81.0	20.9	17.1	65
P4	CF-8M	Pipe	580 OD 32 wall	0.040	0.151	1.07	1.02	10.00	19.64	2.05	83.1	5.9	10.4	182
68	CF-8	Slab	610 x 610 x 76	0.060	0.062	0.62	1.03	8.04	20.53	0.28	84.6	14.8	23.4	87
69	CF-3	Slab	610 x 610 x 76	0.021	0.027	0.62	1.10	8.54	20.14	0.31	83.7	21.4	23.6	35
74	CF-8M	Slab	610 x 610 x 76	0.064	0.048	0.54	0.73	9.03	19.11	2.51	85.8	15.5	18.4	90
75	CF-8M	Slab	610 x 610 x 76	0.063	0.056	0.47	0.61	8.88	20.76	2.30	89.5	23.7	27.8	73
KRB	CF-8	Pump Cover Plate		0.062	0.038	0.31	1.17	8.03	21.99	0.17	-	27.7	-	-

TABLE II. Values of the Constants Representing the Kinetics of Embrittlement for Cast Stainless Steel

Heat	Constants				Activation Energy (kcal/mole)
	K_m (J/cm^2)	β (J/cm^2)	θ	α	
47	163.6	38.5	2.[illegible]	1.11	21.90
51	153.0	31.0	3.06	0.58	44.06
56	100.4	51.3	4.22	1.05	56.05
59	91.2	63.5	3.26	1.55	46.94
60	64.7	63.9	2.82	0.63	47.51
63	140.2	58.4	2.43	0.92	24.30
64	53.3	73.9	2.47	0.66	34.06
65	54.3	78.9	2.84	1.07	36.39
66	94.9	74.9	2.72	1.73	30.23

TABLE III. Values of the Constants in Eq. (3) for Ductile-to-Brittle Transition Curve for Cast Stainless Steels

Heat	Aging Condition		Constants			
	Temp. (°C)	Time (h)	K_o (J/cm^2)	B (J/cm^2)	C (°C)	D (°C)
69	Unaged	-	40	130.34	-186.74	222.03
	320	10,000		78.56	-191.22	5.33
	350	10,000		74.32	-17.43	41.07
	400	2,570		54.29	-45.79	51.20
	400	10,000		55.53	-1.05	87.47
	450	2,570		48.49	-107.84	104.34
I	Unaged	-	50	62.71	-328.09	182.38
	350	9,980		48.96	-117.63	7.58
	400	9,980		47.04	-78.09	84.96
68	Unaged	-	15	133.94	-61.47	110.48
	320	10,000		97.36	-40.89	45.97
	350	10,000		98.30	29.64	64.12
	400	2,570		70.38	34.65	70.83
	400	10,000		65.46	57.54	75.62
	450	2,570		51.49	34.28	41.04
74	Unaged	-	15	89.54	-177.55	119.54
	320	10,000		91.07	-94.95	65.49
	350	10,000		71.40	-39.79	77.57
	400	2,570		61.55	-37.18	49.59
	400	10,000		65.58	19.20	123.65
	450	2,570		39.19	-46.99	63.52
75	Unaged	-	15	90.22	-158.27	42.33
	320	10,000		90.36	-16.13	37.90
	350	10,000		72.63	102.56	113.50
	400	2,570		52.29	47.19	73.84
	400	10,000		64.64	129.44	123.04
	450	2,570		33.46	16.80	93.04
KRB	284	68,000	8	119.70	36.81	83.22
	Reannealed			161.89	-16.54	87.20

TABLE IV. Theoretical Chemical Composition and Ferrite Morphology of Cast Stainless Steel used for Predicting the Extent of Embrittlement under LWR Conditions

Heat	Grade	Composition (wt %)							Ferrite		Q[c] (kcal/mole)	K_m[d] (J/cm^2)
		C	N	Mn	Si	Ni	Cr	Mo	Content[a] (%)	Intercept[b] (μm)		
A	CF-8M	0.05	0.02	1.2	1.2	10.0	21.0	2.6	28	180	18	20
B	CF-8M	0.05	0.05	0.5	1.0	9.0	19.5	2.0	15	80	40	90
C	CF-8	0.04	0.02	1.3	0.5	8.4	21.0	0.4	24	200	18	30
D	CF-8	0.05	0.05	0.5	1.0	8.5	20.5	0.4	15	80	45	90
E	CF-8	0.04	0.02	1.3	0.5	8.4	21.0	0.4	24	200	45	30

[a]Calculated from chemical composition with Hull's equivalent factor.
[b]Assumed values.
[c]Calculated from Eq. (4), value for heat E was assumed.
[d]Determined from Fig. 12.

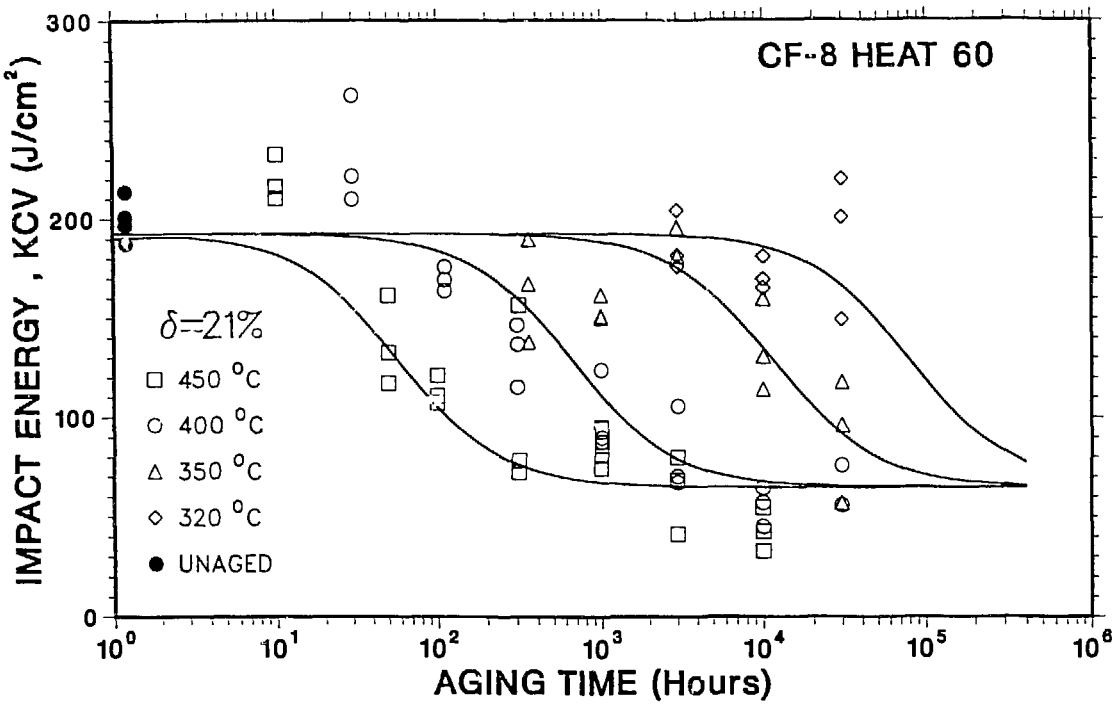

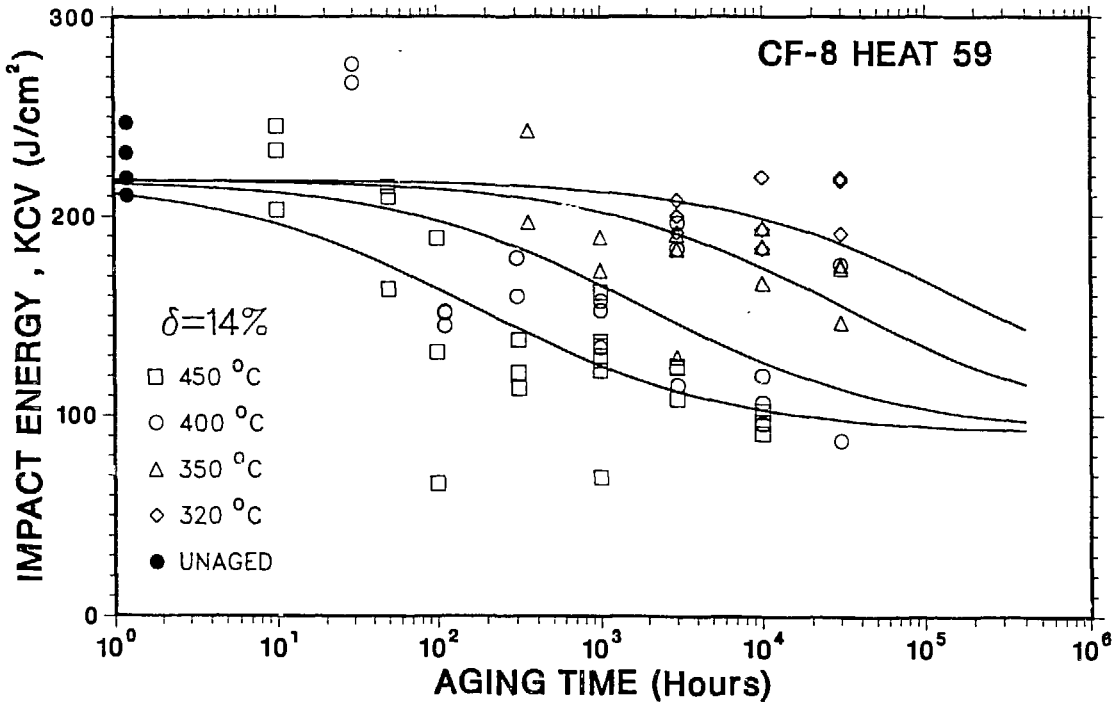

Fig. 1. Effect of Aging Time and Temperature on the Room Temperature Impact Energy of CF-8 Cast Stainless Steel.

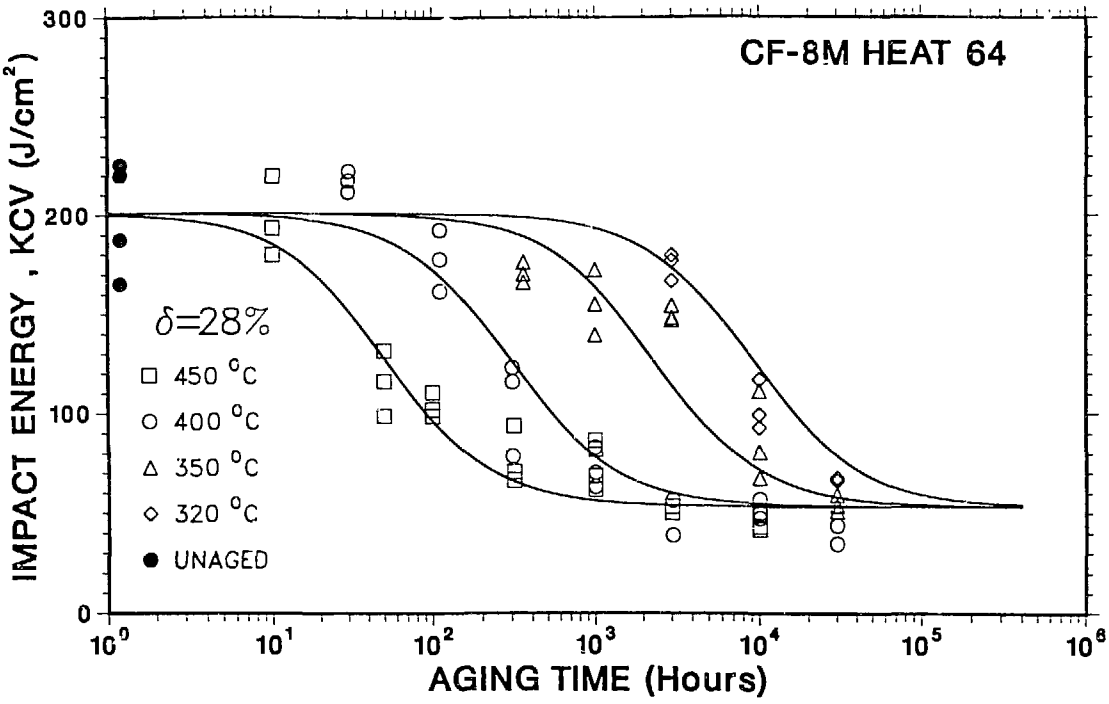

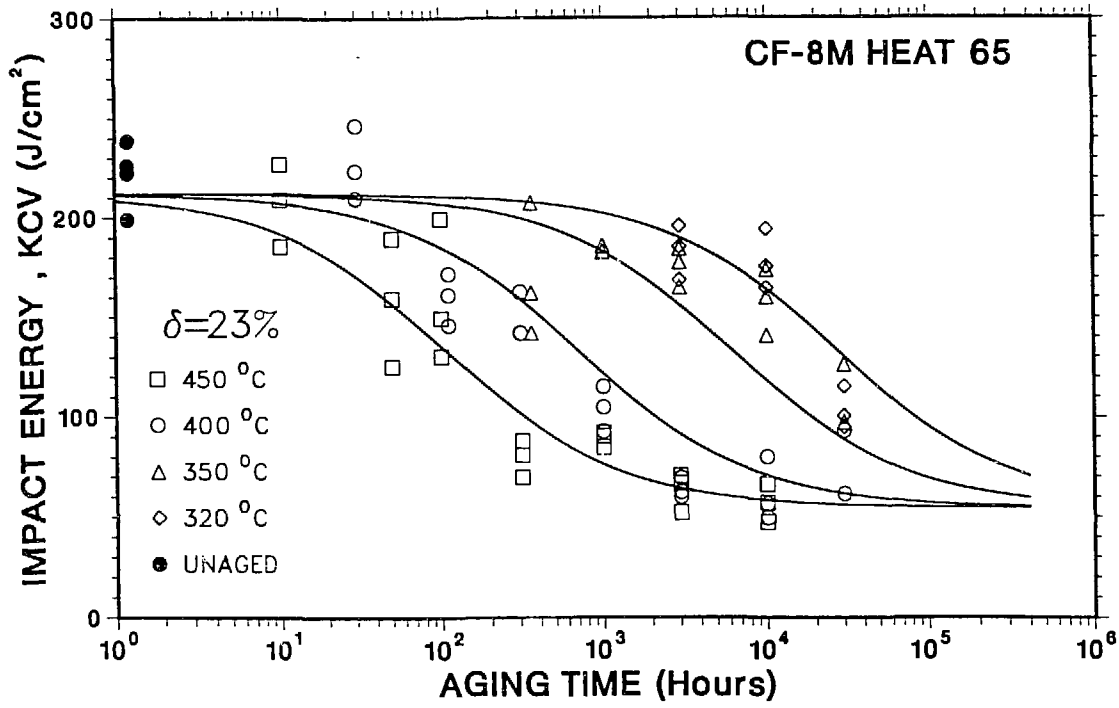

Fig. 2. Effect of Aging Time and Temperature on the Room Temperature Impact Energy of CF-8M Cast Stainless Steel.

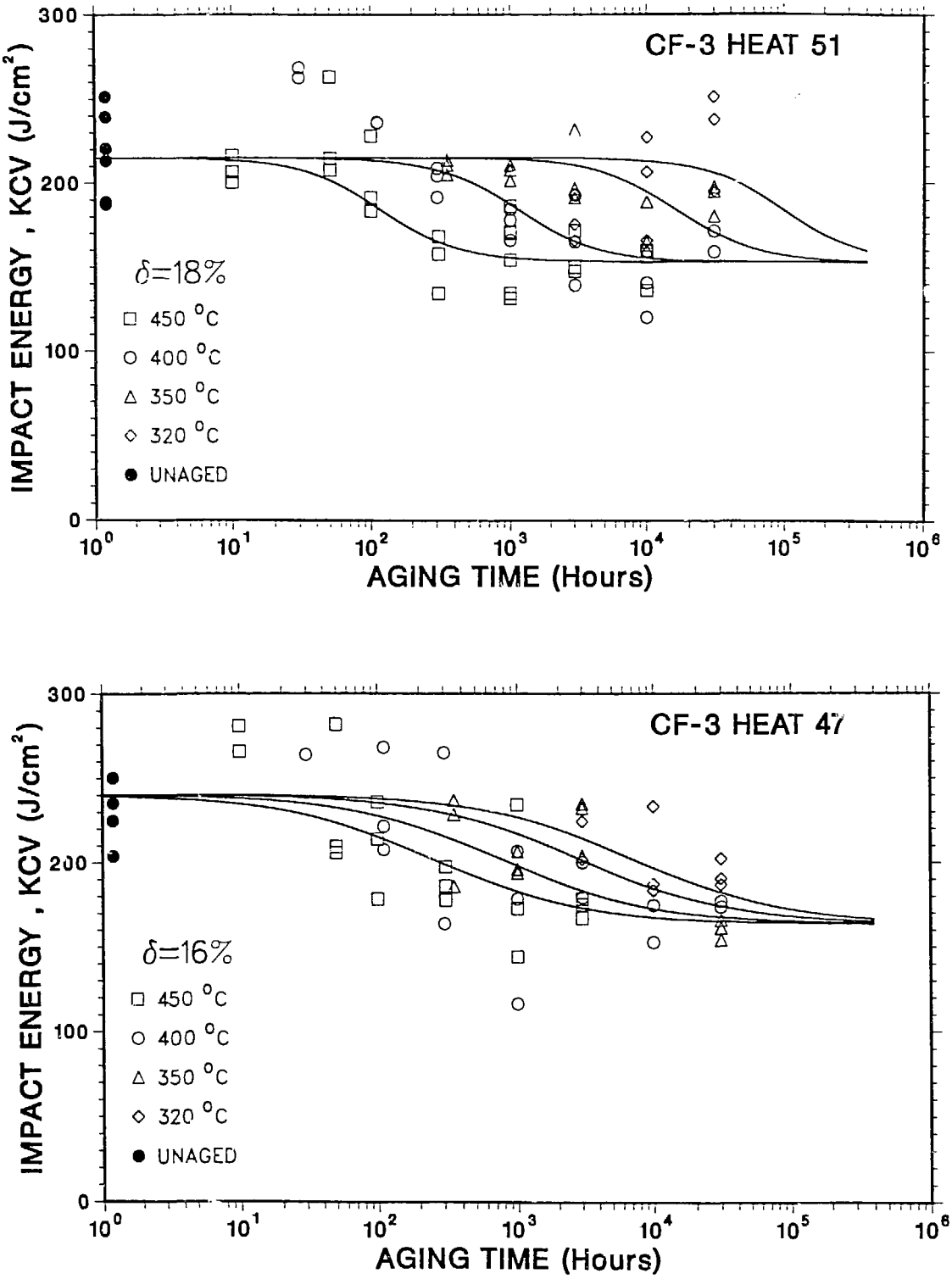

Fig. 3. Effect of Aging Time and Temperature on the Room Temperature Impact Energy of CF-3 Cast Stainless Steel.

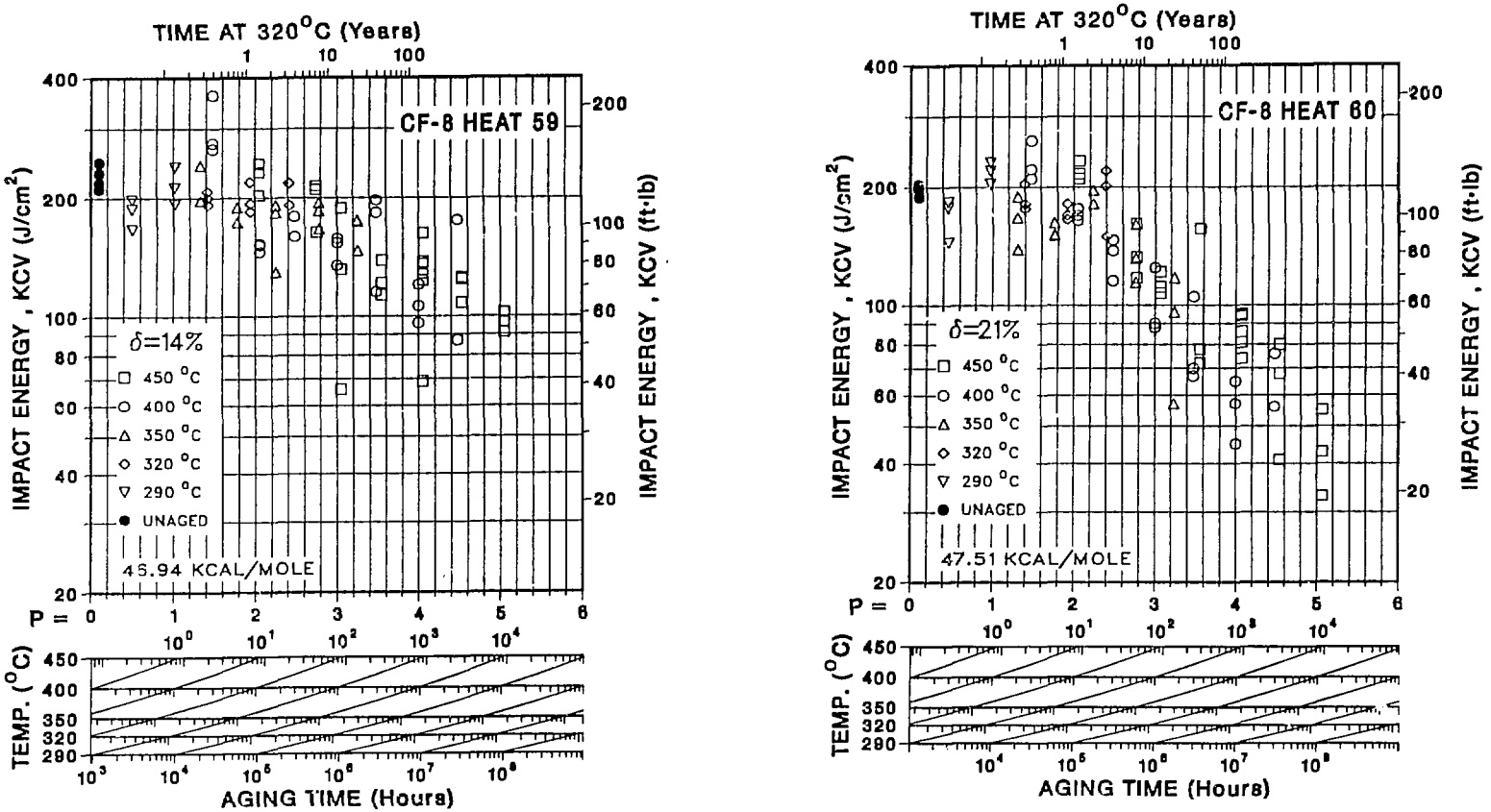

Fig. 4. Influence of Thermal Aging on the Room Temperature Impact Energy of CF-8 Cast Stainless Steel.

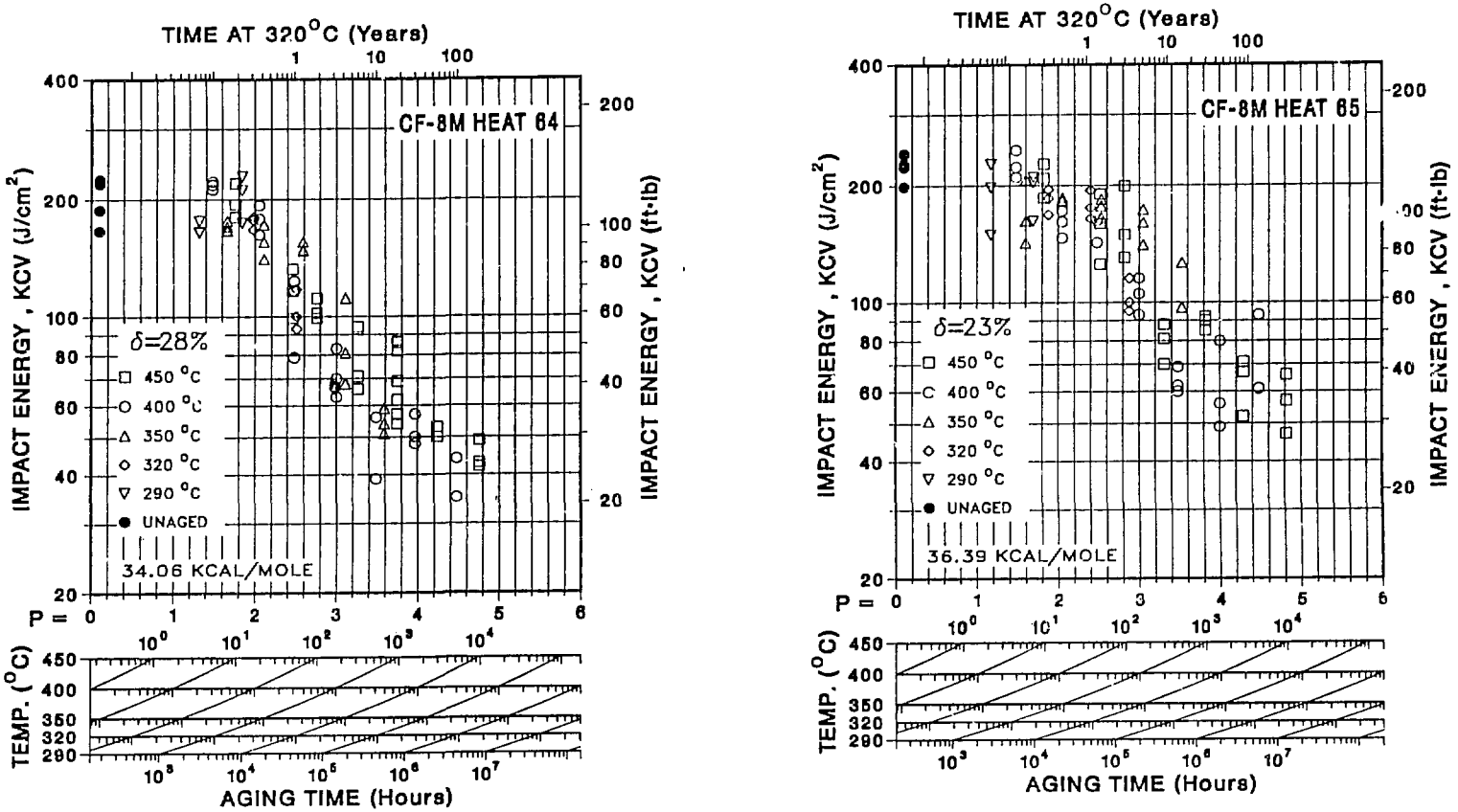

Fig. 5. Influence of Thermal Aging on the Room Temperature Impact Energy of CF-8M Cast Stainless Steel.

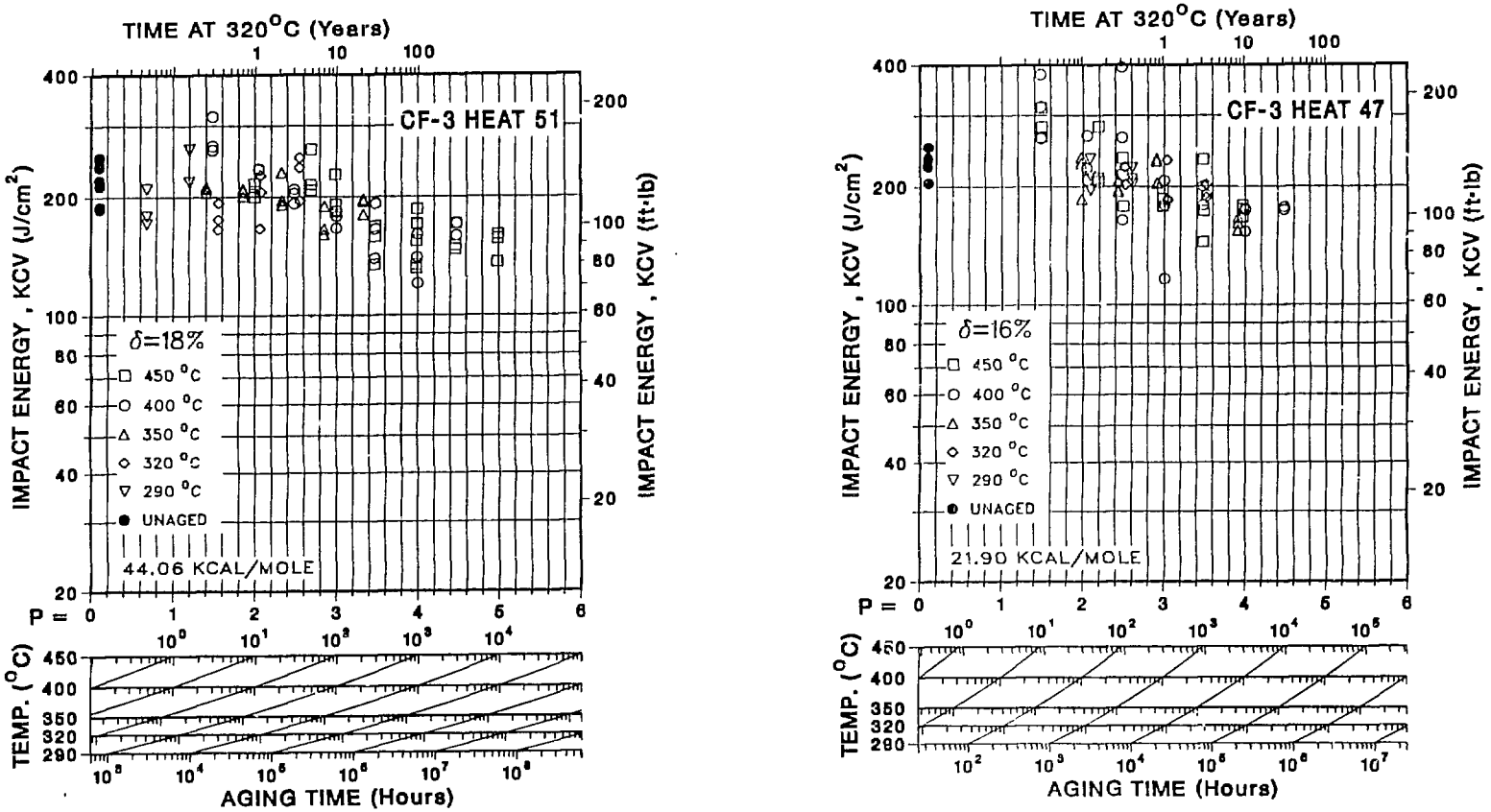

Fig. 6. Influence of Thermal Aging on the Room Temperature Impact Energy of CF-3 Cast Stainless Steel.

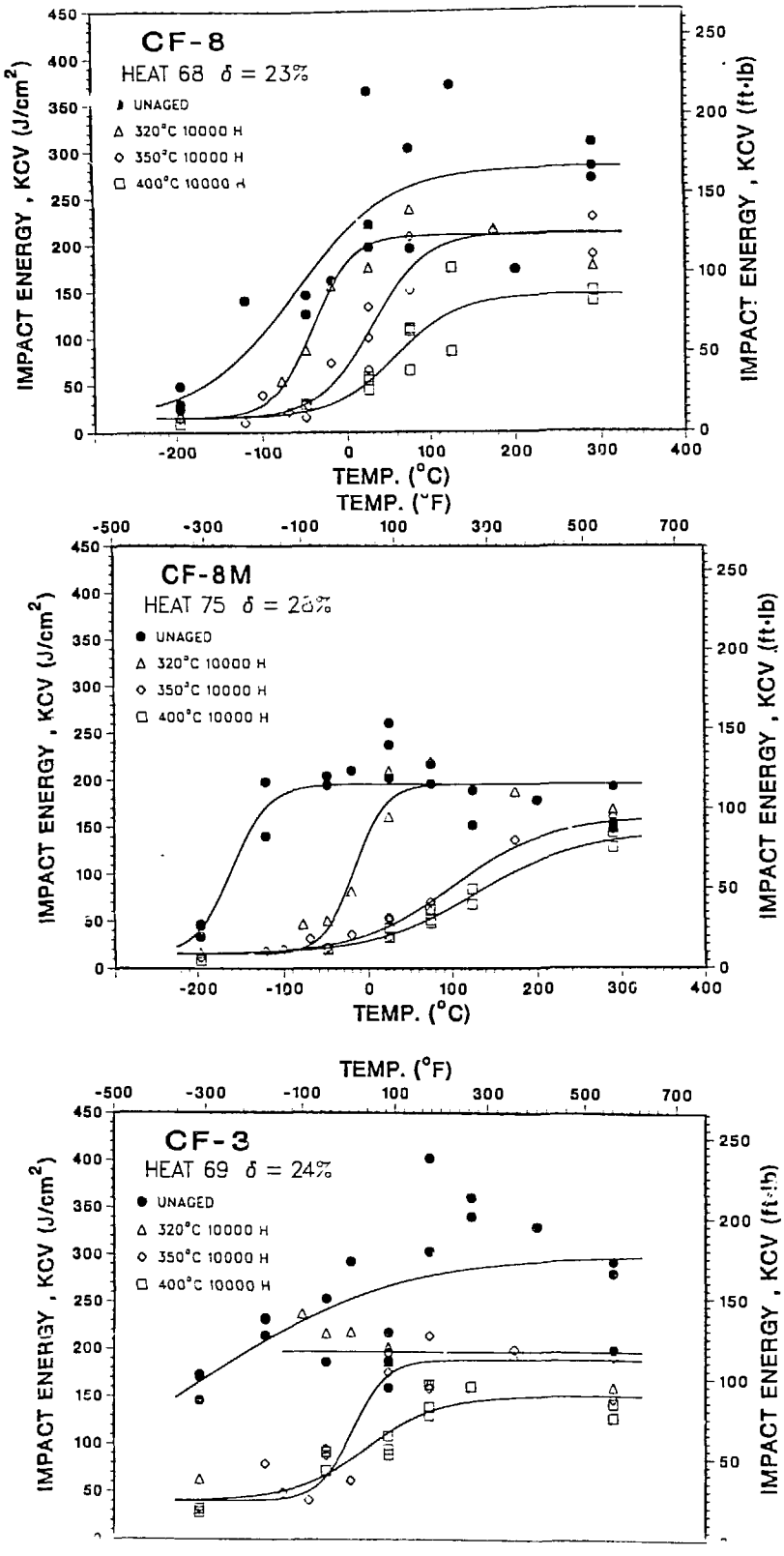

Fig. 7. Effect of Aging Temperature on the Ductile-to-Brittle Transition Curves for CF-8, CF-8M, and CF-3 Grades of Cast Stainless Steel.

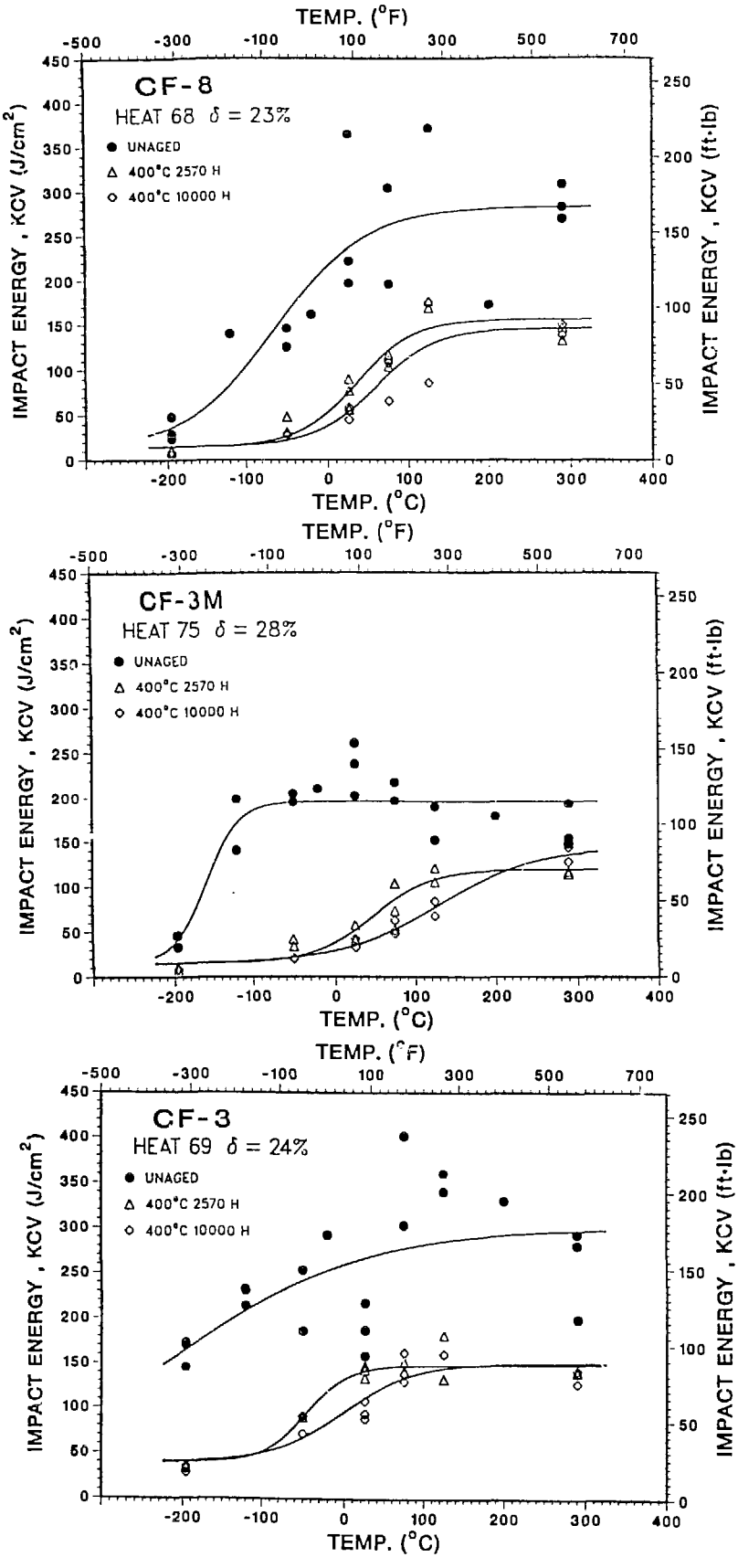

Fig. 8. Effect of Aging Time on the Ductile-to-Brittle Transition Curves for CF-8, CF-8M, and CF-3 Grades of Cast Stainless Steel.

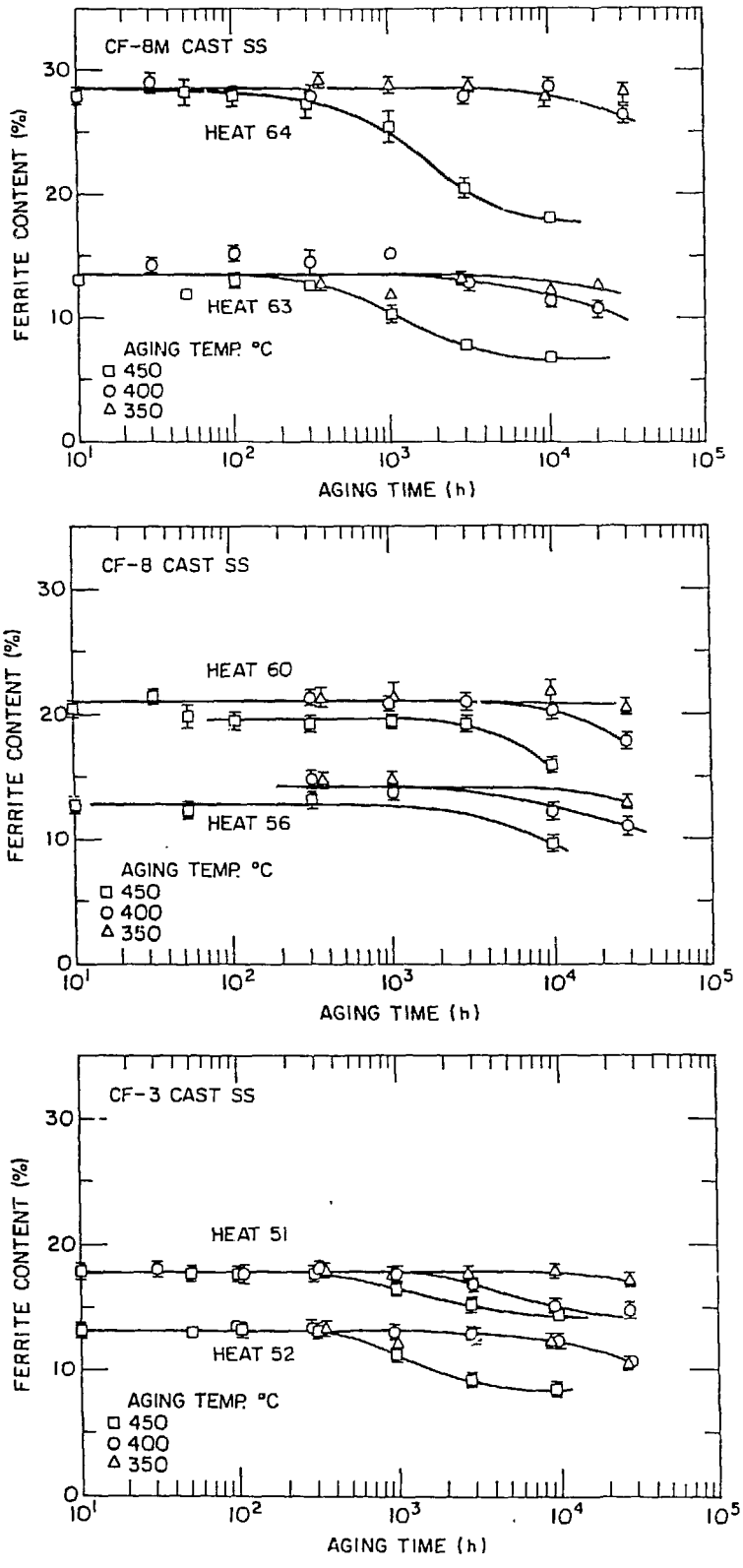

Fig. 9. Decrease in Ferrite Content of Thermally Aged CF-8M, CF-8, and CF-3 Cast Stainless Steel.

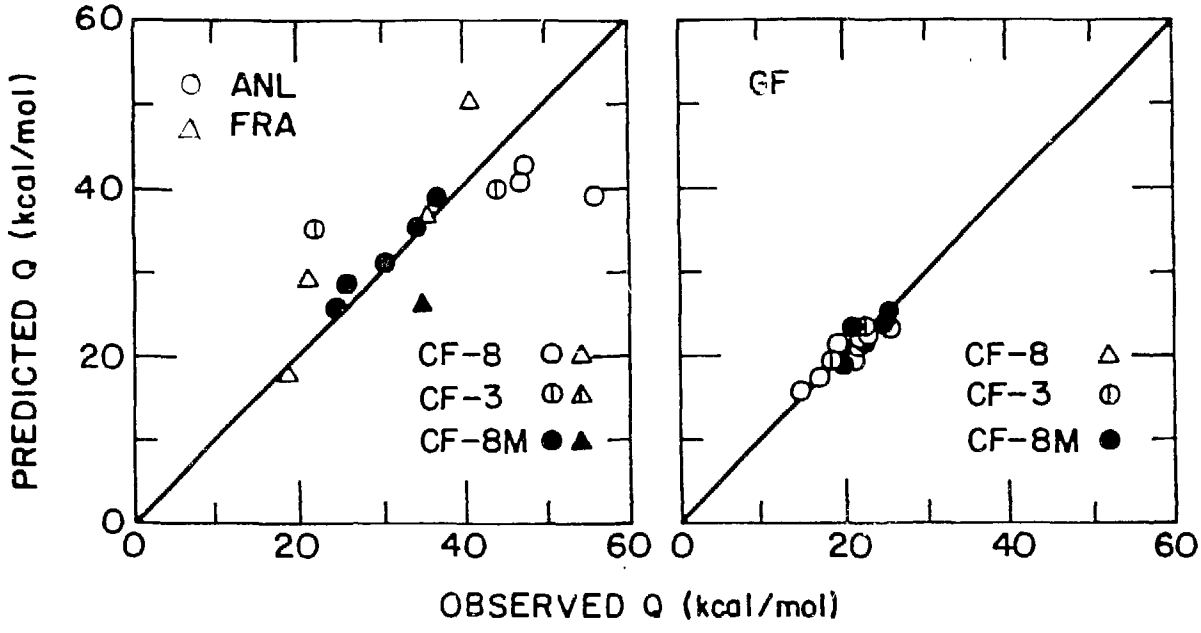

Fig. 10. Observed and Predicted Activation Energy for Low-Temperature Embrittlement of Cast Stainless Steel. ANL: Argonne National Laboratory, FRA: Framatome (Ref. 11), and GF: Georg Fischer Co. (Ref. 1).

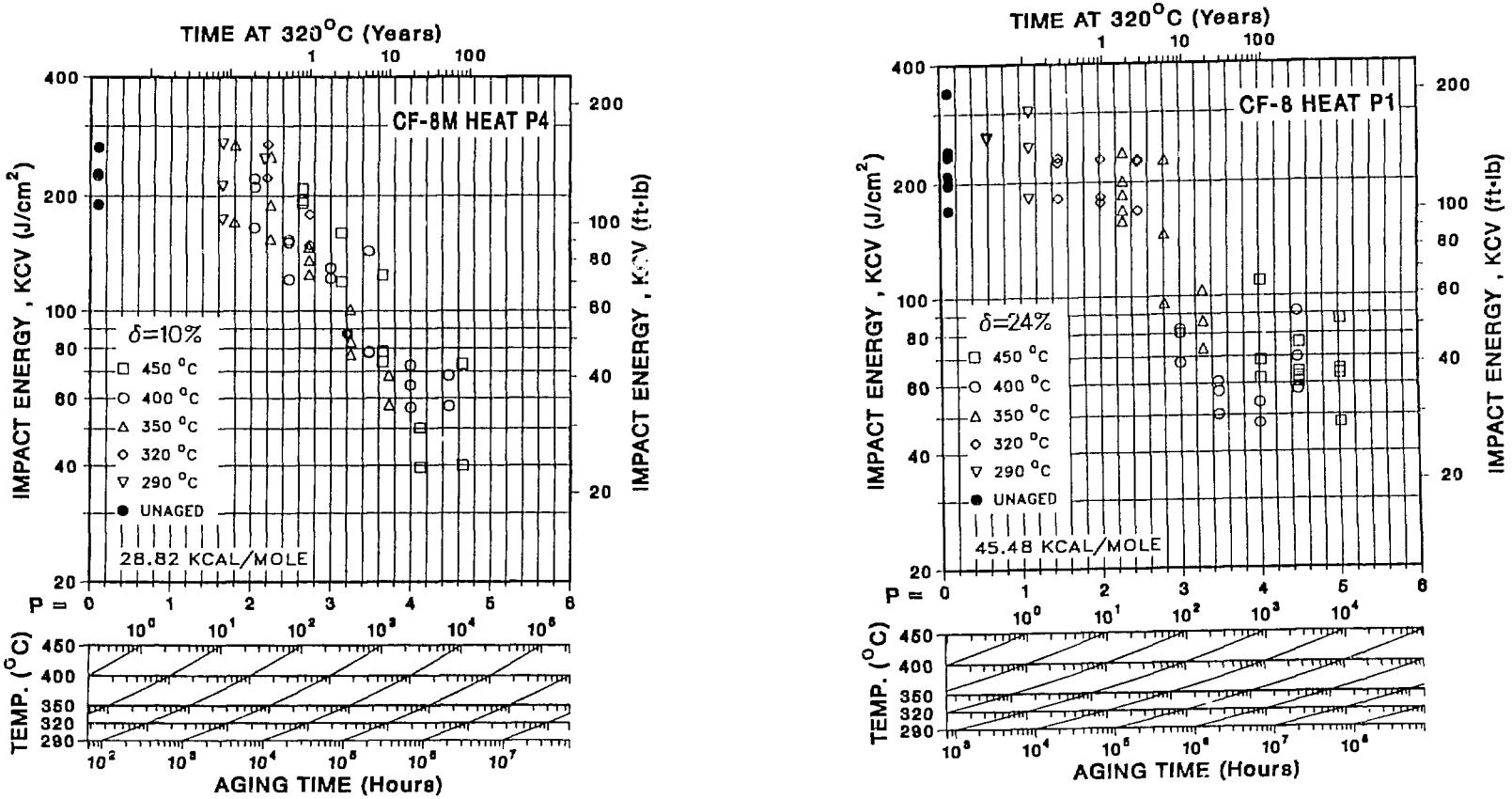

Fig. 11. Impact Energy vs Aging Parameter Curves Based on Calculated Activation Energy for CF-8M and CF-8 Cast Stainless Steel.

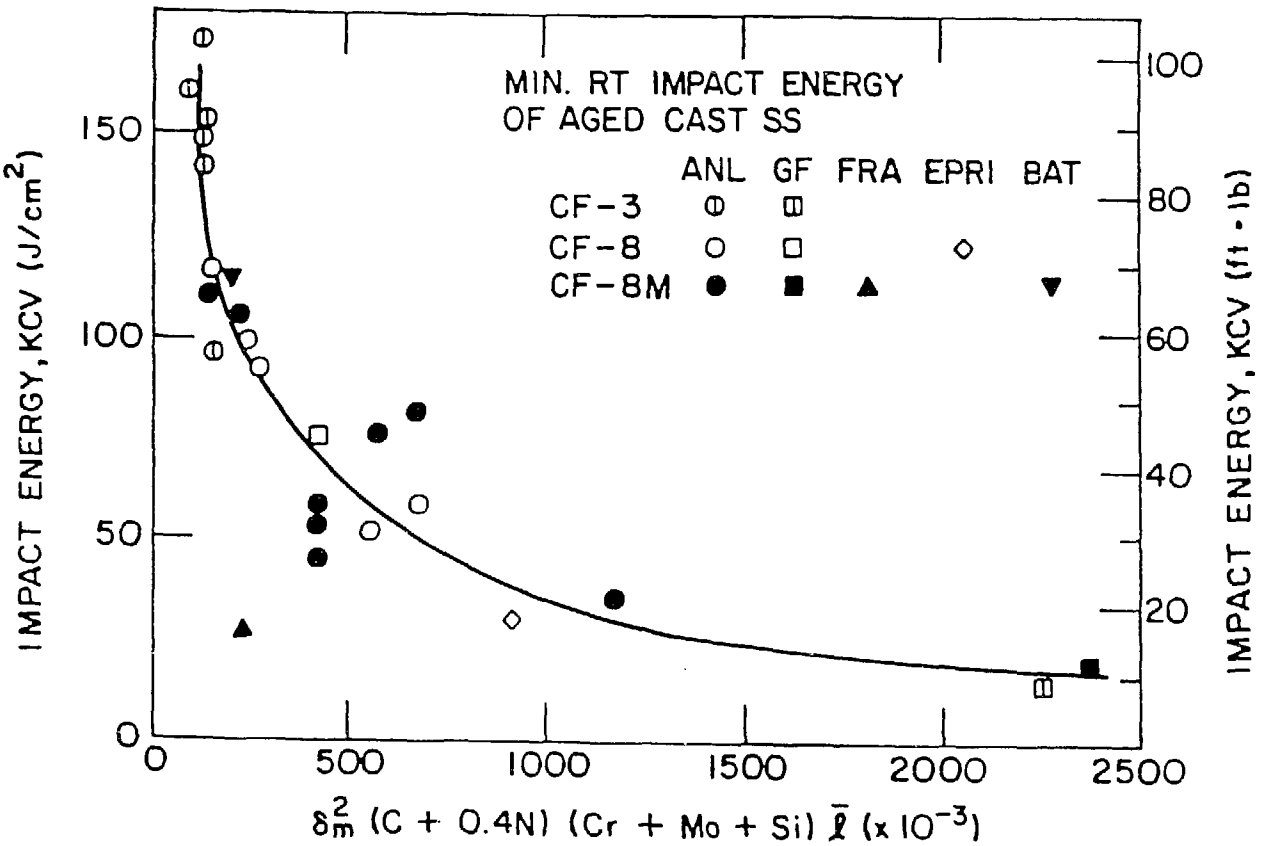

Fig. 12. Correlation between Minimum Room Temperature Impact Energy and Material Parameter for Aged Cast Stainless Steel. EPRI: Electric Power Research Institute (Ref. 17), BAT: Battelle Columbus Division.

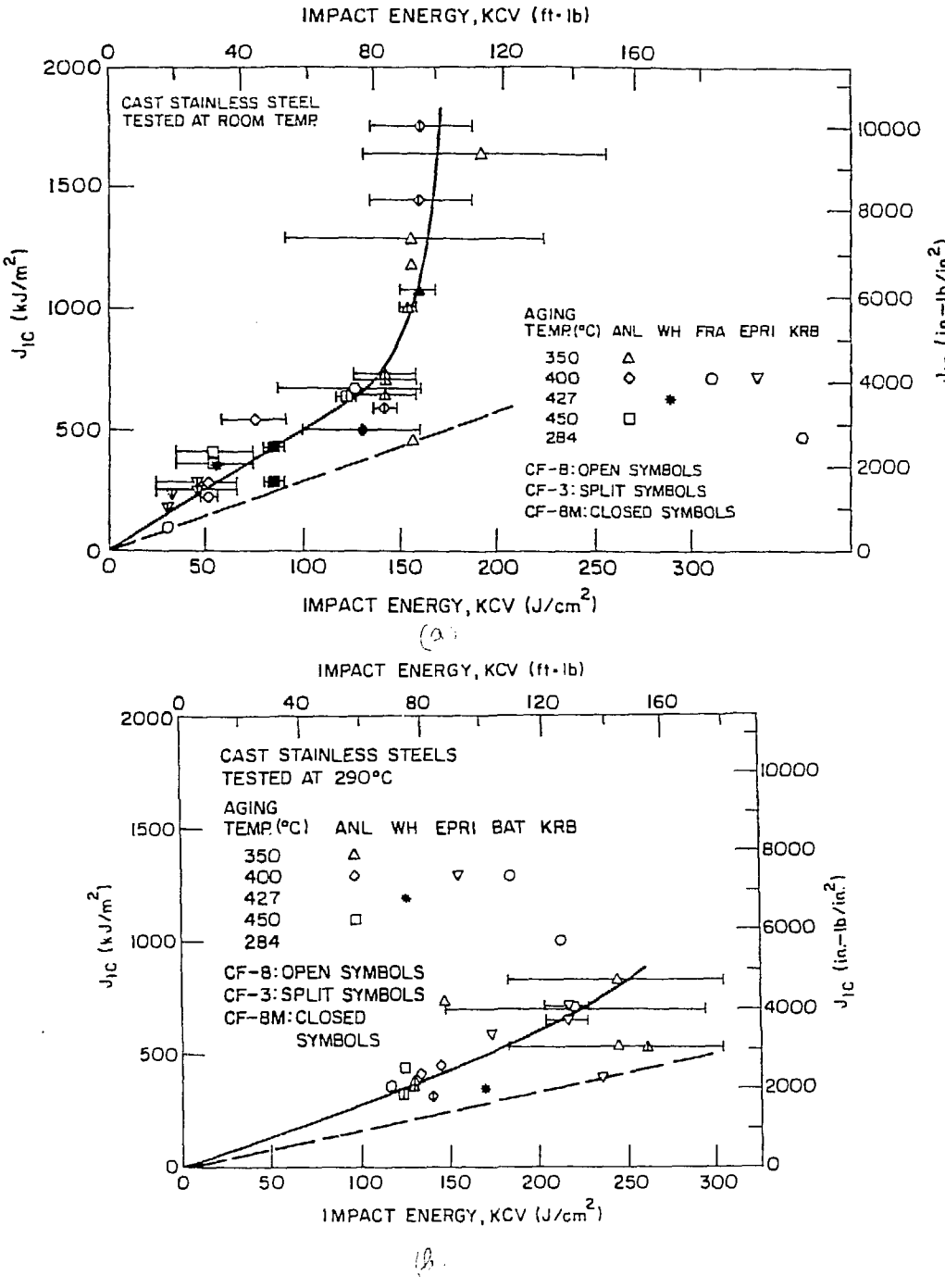

Fig. 13. Correlation between J_{IC} and Impact Energy for Aged Cast Stainless Steel Tested at Room Temperature and at 290°C. WH: Westinghouse (Ref. 19).

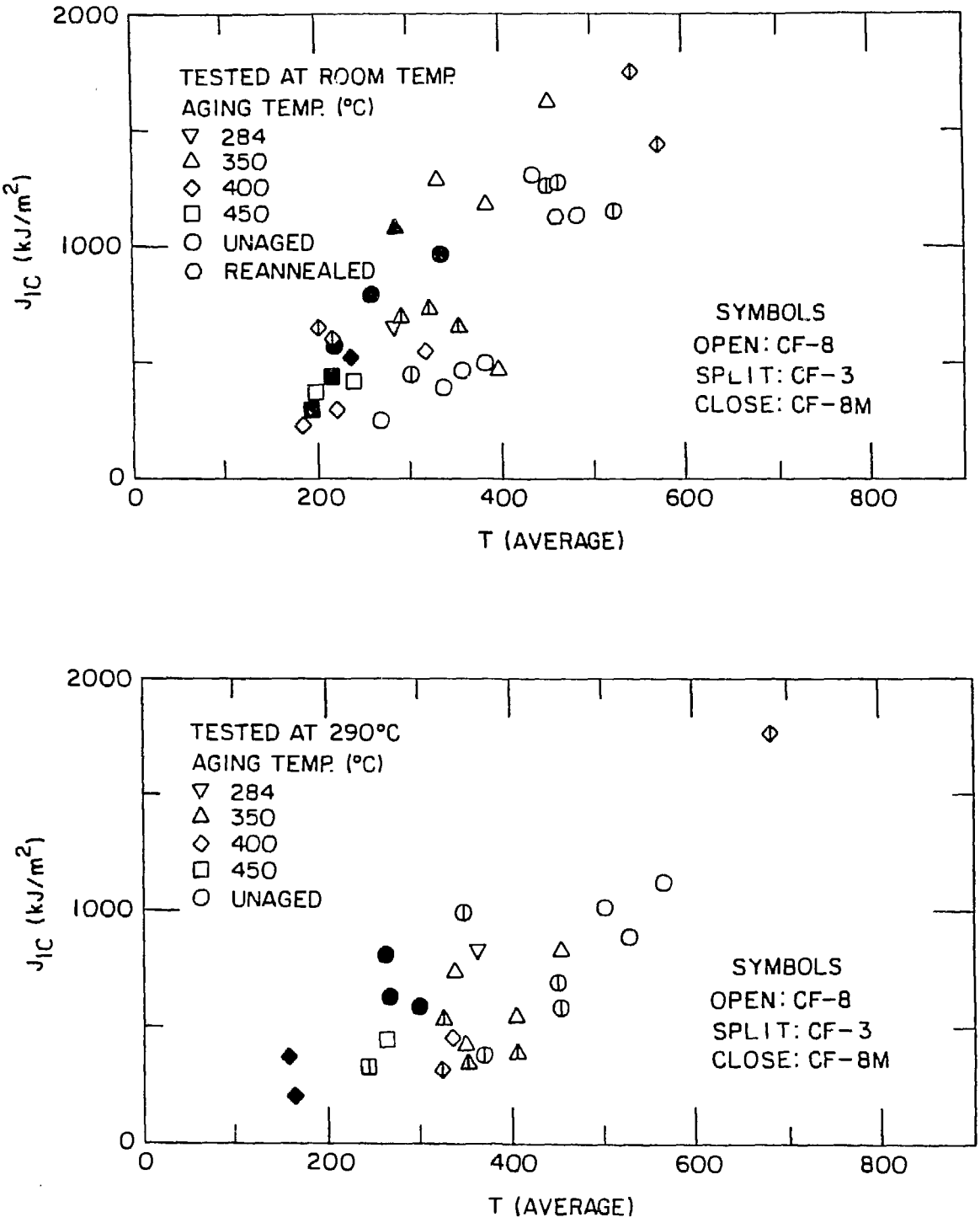

Fig. 14. Correlation between J_{IC} and Tearing Modulus for Cast Stainless Steel Tested at Room Temperature and 290°C.

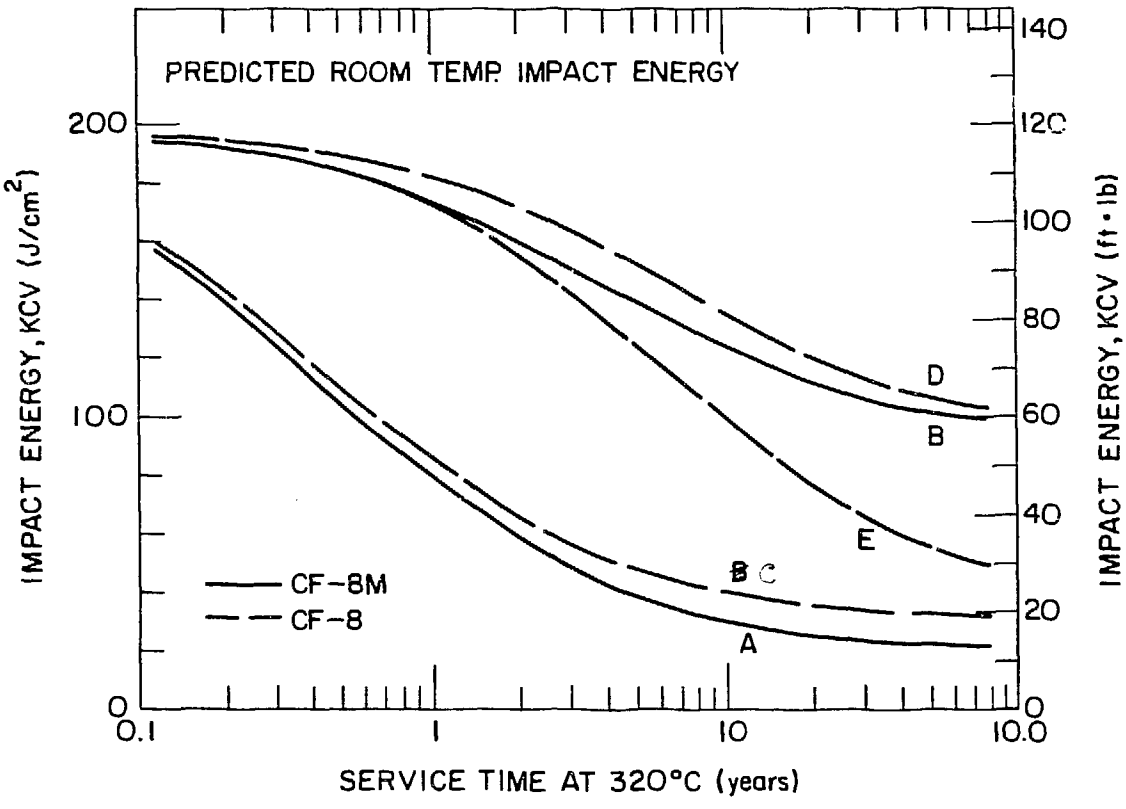

Fig. 15. Predicted Embrittlement Behavior of CF-8M and CF-8 Cast Stainless Steel.

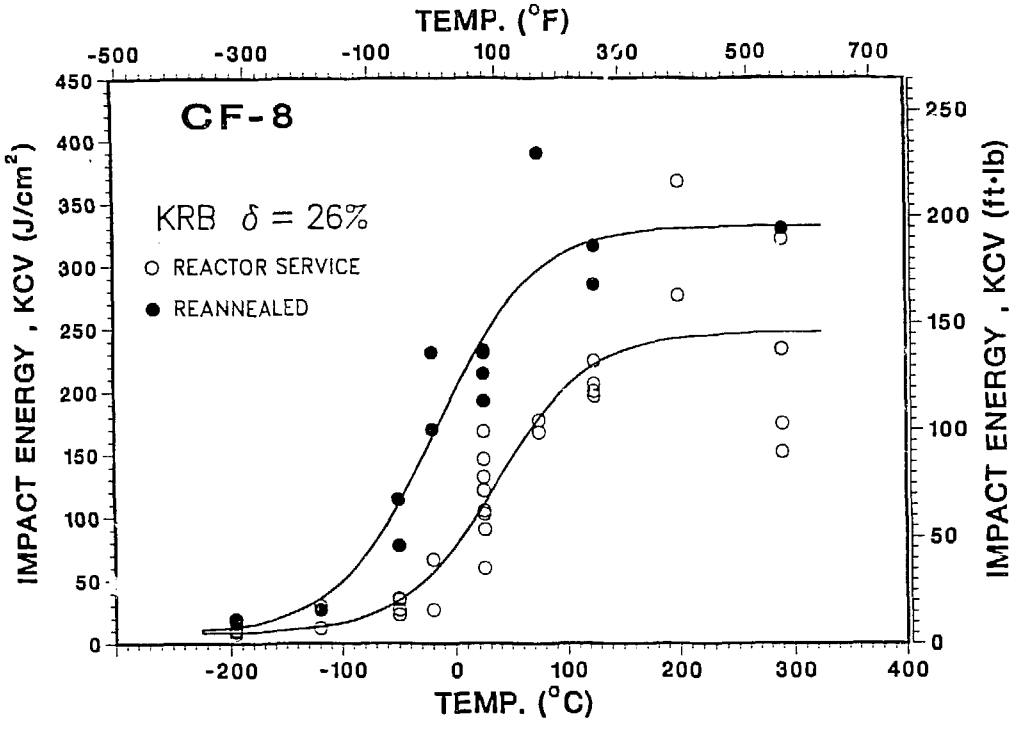

Fig. 16. Effect of Reannealing on the Ductile-to-Brittle Transition Curve for the KRB Pump Cover Plate Material.

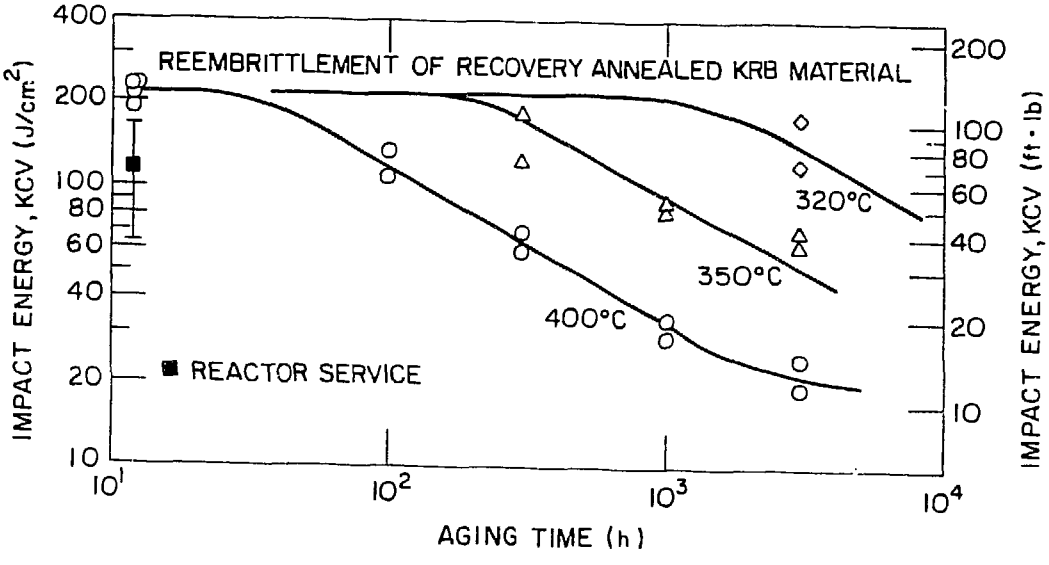

Fig. 17. Reembrittlement Behavior of Recovery Annealed KRB Pump Cover Plate Material.